


# Evapotranspiration and crop coefficient of 'Kent' mango in an important fruit-growing hub in Brazil

Marcelo José da Silva<sup>1,2</sup> | Magna Soelma Beserra de Moura<sup>3,4</sup> |  
 Herica Fernanda de Sousa Carvalho<sup>5</sup> | Cloves Vilas Boas dos Santos<sup>5</sup> |  
 Mário de Miranda Villas Boas Ramos Leitão<sup>2</sup> |  
 Luis Fernando de Souza Magno Campeche<sup>6</sup> | Thieres George Freire da Silva<sup>7</sup> 

<sup>1</sup>Universidade Federal Rural de Pernambuco, Recife, Pernambuco, Brazil

<sup>2</sup>Universidade Federal do Vale do São Francisco, Juazeiro, Bahia, Brazil

<sup>3</sup>Empresa Brasileira de Pesquisa Agropecuária, Embrapa Semiárido, Petrolina, Pernambuco, Brazil

<sup>4</sup>Empresa Brasileira de Pesquisa Agropecuária, Embrapa Agroindústria Tropical, Fortaleza, Ceará, Brazil

<sup>5</sup>Universidade Federal de Pernambuco, Recife, Pernambuco, Brazil

<sup>6</sup>Instituto Federal do Sertão Pernambucano, Petrolina, Pernambuco, Brazil

<sup>7</sup>Unidade Acadêmica de Serra Talhada, Universidade Federal Rural de Pernambuco, Serra Talhada, Brazil

## Correspondence

Thieres George Freire da Silva, Unidade Acadêmica de Serra Talhada, Universidade Federal Rural de Pernambuco, Av. Gregório Ferraz Nogueira, S/N, José Tomé de Souza Ramos, CEP: 56909-535, Serra Talhada/PE Caixa, 063, Brazil.  
 Email: [thieres.silva@ufrpe.br](mailto:thieres.silva@ufrpe.br)

## Funding information

Coordenação de Aperfeiçoamento de Pessoal de Nível Superior, Grant/Award Number: Finance Code 001; Conselho Nacional de Desenvolvimento Científico e Tecnológico, Grant/Award Number: 309421/2018-7

## Abstract

The 'Kent' mango is one of the main cultivars produced in the São Francisco valley. However, due to a lack of data, water management was carried out using coefficients from the Tommy Atkins cultivar. Thus, aiming to achieve greater water management efficiency, the aim of this study was to evaluate the growth, radiation and energy balance, evapotranspiration and coefficients of the 'Kent' mango in the lower-middle São Francisco valley in Brazil. The study was conducted in an orchard over two harvests between 2017 and 2018. The radiation and energy balance, evapotranspiration ( $ET_c$ ) and crop coefficients ( $K_c$ ) of the mango were estimated from micrometeorological data. The mean reference evapotranspiration ( $ET_0$ ) and  $ET_c$  values were 5.47 and 4.40 mm day<sup>-1</sup> (vegetative growth, VG), 4.42 and 4.29 mm day<sup>-1</sup> (floral induction, FI), 4.08 and 3.48 mm day<sup>-1</sup> (floral induction + flowering, FI + FL), 4.51 and 3.63 mm day<sup>-1</sup> (fruit drop, FD) and 6.09 and 4.46 mm day<sup>-1</sup> (formation fruit + maturation fruit phase, FF + MF). Under the climate conditions of the São Francisco valley,  $K_c$  values of 0.80, 0.97, 0.85, 0.80 and 0.74 are recommended for the 'Kent' mango during the VG, FI, FI + FL, FD and FF + MF phases, respectively.

## KEYWORDS

Bowen ratio, irrigation management, *Mangifera indica* L

## Résumé

La mangue 'kent' est l'un des principaux cultivars produits dans la vallée de Francisco. Cependant, en raison d'un manque de données, la gestion de l'eau a été effectuée à l'aide des coefficients du cultivar Tommy Atkins. Ainsi, dans le but d'atteindre une plus grande efficacité de la gestion de l'eau, le but de cette étude était d'évaluer la croissance, le rayonnement et le bilan énergétique, l'évapotranspiration et les coefficients de la mangue 'kent' dans la vallée moyenne inférieure de Francisco au Brésil. L'étude a été menée dans un verger

sur deux récoltes entre 2017 et 2018. Le rayonnement et le bilan énergétique, l'évapotranspiration ( $ET_c$ ) et les coefficients de culture ( $K_c$ ) de la mangue ont été estimés à partir de données micrométéorologiques. Les valeurs d'évapotranspiration de référence moyenne ( $ET_0$ ) et  $ET_c$  étaient de 5,47 et 4,40 mm jour<sup>-1</sup> (croissance végétative, VG), 4,42 et 4,29 mm jour<sup>-1</sup> (induction florale, FI), 4,08 et 3,48 mm jour<sup>-1</sup> (induction florale + floraison, FI + FL), 4,51 et 3,63 mm jour<sup>-1</sup> (goutte de fruit, FD) et 6,09 et 4,46 mm jour<sup>-1</sup> (formation fruit + phase de maturation du fruit, FF + MF). Dans les conditions climatiques de la vallée de Francisco, des valeurs  $K_c$  de 0,80, 0,97, 0,85, 0,80 et 0,74 sont recommandées pour la mangue «Kent» pendant les phases VG, FI, FI + FL, FD et FF + MF, respectivement.

#### MOTS CLÉS

*Mangifera indica* L, gestion de l'irrigation, rapport de Bowen

## 1 | INTRODUCTION

Irrigated agriculture has been strongly influenced by the water crisis caused by climate change (Zuazo et al., 2019). These conditions cause producers to look for alternatives that minimize negative impacts on production (Simões et al., 2021). In regions where water scarcity and poor spatiotemporal distribution of rainfall affect crop development, the use of efficient irrigation management is essential (Coelho et al., 2008; Cotrim et al., 2017).

In Brazil, for example, the irrigated area already exceeds 8.2 million ha, with the prospect of an increase of another 4.2 million ha by 2040 (Agência Nacional de Águas [ANA], 2021). However, although these numbers demonstrate advances from a technological point of view, the management of water resources still needs attention, as water is a scarce and important resource for the sustainability of crops, especially in semi-arid regions.

Among the activities carried out in the country, irrigated fruit growing is considered one of the most profitable; however, its territorial expansion combined with the regional water crisis revealed the need to employ strategic methodologies (i.e. crop evapotranspiration [ $ET_c$ ], energy balance, soil moisture and/or phenological phases) to manage the soil–water–plant system (Silva et al., 2009; Simões et al., 2018), considering that the agricultural sector is responsible for the consumption of 70% of fresh water (Calzadilla et al., 2010). Therefore, for this objective to be achieved, it is necessary for the producer/irrigator to have information about the culture, climate and soil of the region.

The water demand or evapotranspiration of a crop can be estimated by methods that involve the radiation balance and surface energy balance, such as the correlation between turbulent vortices and the energy balance

based on the Bowen ratio (EBBR) (Campeche et al., 2011; Silva et al., 2015). These methods are based on partitioning the net radiation ( $R_n$ ) into latent heat flux (LE), sensible heat flux ( $H$ ) and soil heat flux ( $G$ ). Another parameter that expresses the water consumption of a crop throughout its cycle is the crop coefficient ( $K_c$ ). This represents the ratio between the crop evapotranspiration ( $ET_c$ ) and the reference evapotranspiration ( $ET_0$ ), which is adopted as an adjustment factor between the atmospheric demand and the crop demand and varies according to the type of management adopted (Pereira et al., 2013). Therefore, the application of these methods in places with high production potential, in addition to promoting better management of water use, can maximize performance considering that the crop will not run the risk of suffering water stress.

The São Francisco valley is an important fruit-producing hub for Brazilian agribusiness. Irrigated fruit farming has favourable climate conditions in the region, which, together with the water regime and the adoption of phytotechnical management technology, have resulted in high levels of production and fruit quality, reaching the most demanding markets in Brazil and the world (Mouco, 2015). Among the fruits exploited in Brazil, mango (*Mangifera indica* L.) has shown excellent results. According to the Brazilian Horti and Fruti Yearbook (2022), mangos are responsible for a revenue of USD248.1 million resulting from the export of 272.5 t of fruit in 2021, which is 12% greater than that of the previous year. In 2022, mango production in Brazil was estimated at 1,546,375 t, especially in the states of Pernambuco and Bahia (Instituto Brasileiro de Geografia e Estatística [IBGE], 2024), particularly for the 'Tommy Atkins', 'Kent', 'Palmer' and 'Keitt' varieties (Figueiredo Neto et al., 2017).

The Kent cultivar is one of the most common cultivars produced in the Vale do São Francisco region (Andrade et al., 2023). With good acceptance on the international market, its fruits have a pleasant flavour, high levels of soluble solids and low amounts of fibre (Barbosa et al., 2023). More recent studies involving this cultivar indicate that its productive characteristics and fruit quality are strongly influenced by the water depth applied at the time of irrigation (Andrade et al., 2023; Simões et al., 2021). However, due to the lack of studies, such management is carried out using specific data from the ‘Tommy Atkins’ cultivar.

Studies carried out to determine the evapotranspiration and crop coefficient of irrigated ‘Tommy Atkins’ mango in the São Francisco valley using the Bowen ratio have shown that LE represents between 77 and 84% of the  $R_n$  (Teixeira, Bastiaanssen, Moura, et al., 2008; Teixeira, Bastiaanssen, Ahmad, et al., 2008). Silva et al. (2007), analysing two irrigated cycles of the same variety in the district of Petrolina, found that the energy used by LE represented, on average, 75–78% of the  $R_n$ , giving an accumulated  $ET_c$  of 784.6 and 719.3 mm between flowering and harvesting, respectively. For the same variety, mean  $K_c$  values of 0.71 and 0.91 were found by Azevedo et al. (2003) and Teixeira, Bastiaanssen, Moura, et al. (2008), respectively. However, differences in morphological characteristics and different adjustments in production management between the ‘Tommy Atkins’ and ‘Kent’ varieties demand specific studies of this cultivar, particularly its water demand, since the cultivar represents one of the largest planted areas in the lower-middle São Francisco valley.

Thus, knowing the relevance of this cultivar for the region, as well as the importance of adopting effective strategies, scientific advances concerning the water demand of the ‘Kent’ cultivar and its relationship to the morphological characteristics of the plant are therefore necessary to generate information that might produce a more efficient form of irrigation management, with longer-lasting water, food and economic security for the region of the São Francisco valley. As such, the aim of this study was to analyse the growth, radiation and energy balance, evapotranspiration and crop coefficient of the ‘Kent’ mango in the lower-middle São Francisco valley to propose technical coefficients for direct application in water management.

## 2 | MATERIALS AND METHODS

### 2.1 | Area and crop under study

The study was carried out in a commercial mango orchard located at the ‘Andorinhas Farm’ (latitude:

9°27′16″ S; longitude: 40°36′55″; 380 m above sea level) in the municipality of Petrolina, Pernambuco state, in the lower-middle São Francisco valley, Brazil (Figure 1). According to the Köppen classification, the climate in the region is type BswH’ (semi-arid), with a rainy period from January to April (Alvares et al., 2013). The soil in the experimental area is classified as sandy, and the properties of the soil are shown in Table S1. The experiment was conducted from 10 June 2017 to 20 October 2018 and included part of the 2016/2017 crop (10 June 2017 to 7 November 2017) and the entire 2017/2018 crop (8 November 2017 to 20 October 2018).

The study area consisted of a plot of 5.01 ha cultivated with ‘Kent’ mango planted 9 years earlier at a spacing of 4 × 6 m (24 m<sup>2</sup>) in an east–west direction (Figure 2). The first cycle under evaluation began on 21 November 2016 with production pruning. This was followed by fertilization with ammonium sulphate, potassium sulphate and organic acid. Paclobutrazol (PBZ) was applied 45–60 days after pruning together with organic acid at doses of 35 ml plant<sup>-1</sup> and 4 L ha<sup>-1</sup>, respectively (during the vegetative growth phase). For the branches to mature, five applications of potassium nitrate (2.5%) and sulphur (0.2%) were applied using a volume of 600 L solution ha<sup>-1</sup> (floral induction phase). Foliar fertilization and fertigation were carried out weekly to meet the need for nitrogen, potassium, phosphorus, calcium, magnesium and boron. Doses of amino acid (0.5%) were applied during the production cycle, following the recommendations of the farm technicians responsible. Fertilization management during the second cycle was similar to that carried out during the first, beginning after the production pruning, which took place on 23 November 2017.

The orchard was irrigated twice daily (approximately 5:00 AM to 7:00 AM and 1:00 PM to 3:00 PM) based on the crop demand adopted by the technicians at the farm and respecting the orchard sectorization logistics. An average daily depth of 4.5 mm was applied, varying according to the behaviour of the meteorological variables and phenological phases. During the floral induction phase (2 March 2018 to 1 July 2018), the culture was subjected to controlled water stress (average daily depth of 2.8 mm). This management approach is important for greater flower/panicle formation and increased productivity. A microsprinkler irrigation system was used, for which field tests indicated a mean flow rate of 24 L h<sup>-1</sup>, resulting in a watering diameter of 4.80 m (18.09 m<sup>2</sup>) at a mean output pressure of 0.4 MPa. The distribution uniformity coefficient (DUC) of the system had a mean value of 80% and was classified as good based on the methodology proposed by Mantovani (2001).



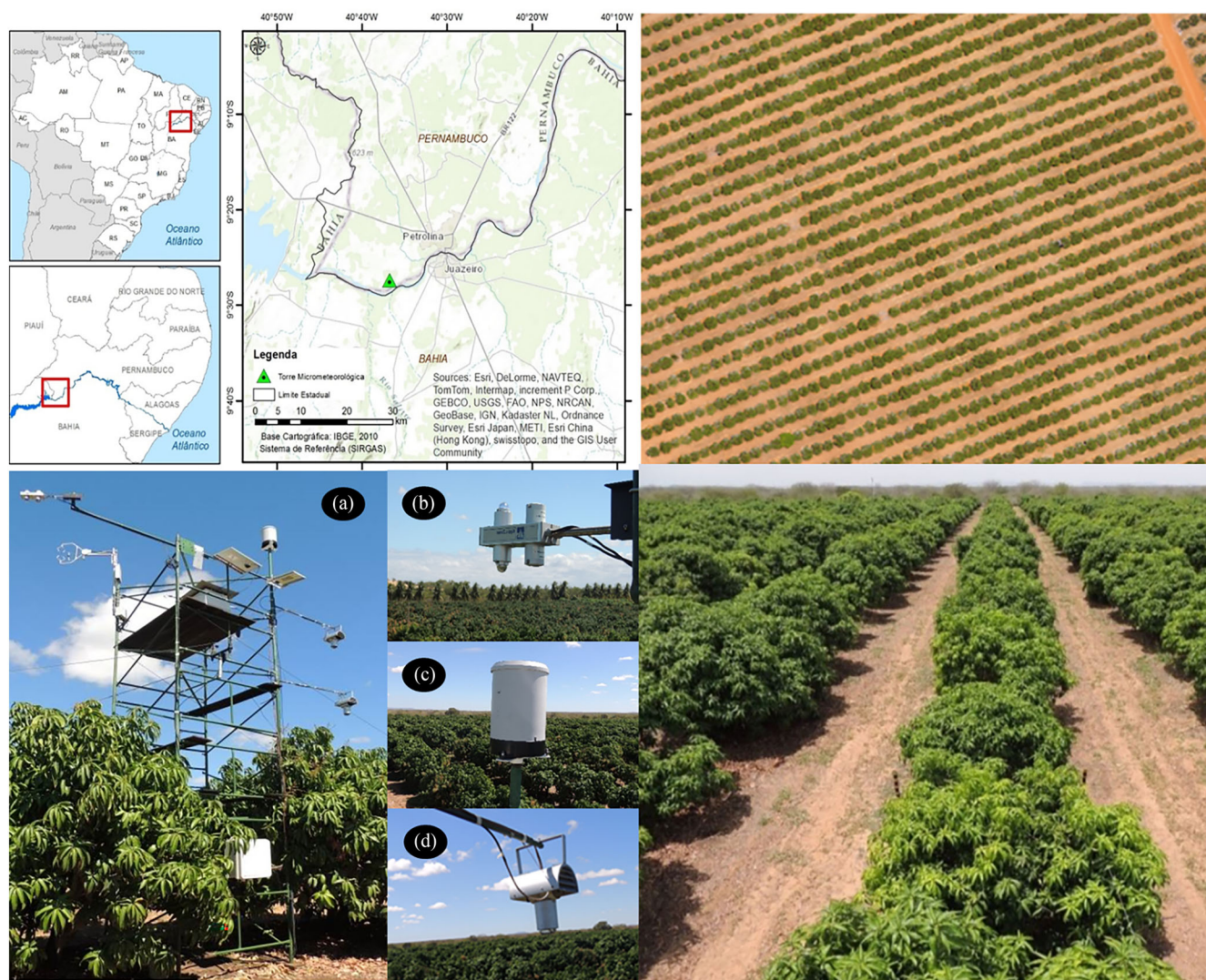


**FIGURE 1** Location of the experimental area (Fazenda Andorinhas Farm) and the micrometeorological tower (a) equipped with sensors [net radiometer (b), rain gauge (c) and psychrometers (d)] to record the climate variables in an irrigated orchard of the ‘Kent’ mango in Petrolina, Pernambuco.

## 2.2 | Phenology and crop growth parameters

### 2.2.1 | Phenology

The phenology and crop growth parameters were determined from the fortnightly monitoring of 10 plants selected from inside the orchard (Figure 2). The phenological phases were analysed by adapting the methodology of Rodrigues et al. (2013), considering the presence of at least 51% of the specific characteristics of each phase. Vegetative growth considered the days between production pruning and the start of panicle emergence; floral induction considered the period of sharp reduction in irrigation depth to stimulate floral

induction; and floral induction + flowering represented the period in which the plants simultaneously presented fully opened panicles and developing panicles. In this case, the floral induction + flowering phase considered the days with a gradual increase in the irrigation depth until the appearance of small pellet-sized fruits. This management was carried out with the aim of obtaining greater efficiency in flowering. The fruit drop phase was considered to begin with the presence of pellet-sized fruit on the plant or on the ground, and the fruit formation + maturation phase was considered to be the period starting with more than pellet-sized fruit until harvest. Table 1 shows the period of each phenological phase under analysis for the two production cycles.



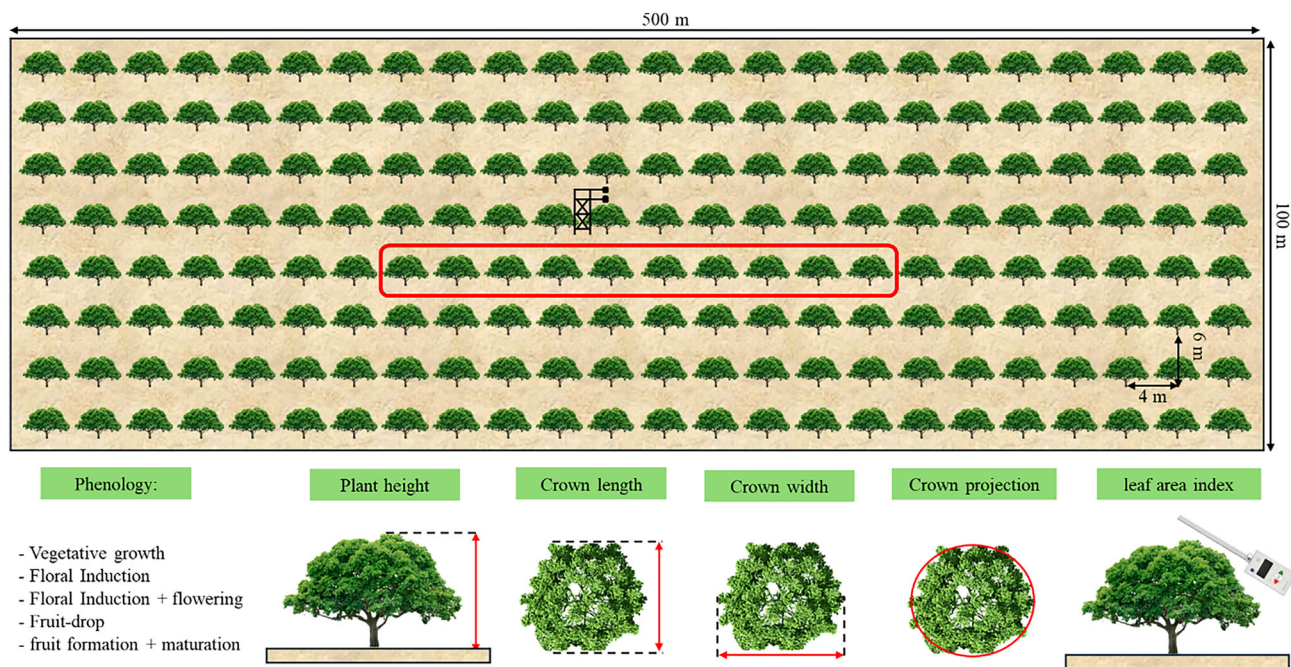


**FIGURE 2** Sketch of the experimental area and representation of biometric measurements in each phenological phase in an irrigated orchard of the ‘Kent’ mango in Petrolina, Pernambuco.

**TABLE 1** Phenological phases of the ‘Kent’ mango grown in the lower-middle São Francisco valley.

Phenology	Cycle 2016–2017	Number of days	Cycle 2017–2018	Number of days
Vegetative growth	–	–	08 November 2017 to 01 March 2018	114
Floral induction	–	–	02 March 2018 to 30 April 2018	60
Floral induction + flowering	–	–	01 May 2018 to 01 July 2018	62
Fruit drop	10 June 2017 to 25 August 2017	77	02 July 2018 to 22 August 2018	52
Fruit formation + fruit maturation	26 August 2017 to 07 November 2017	74	23 August 2018 to 20 October 2018	59

### 2.2.2 | Plant height, crown diameter and projection

Crop growth was evaluated every 2 weeks in biometric campaigns to measure plant height ( $PH$ , m) and crown diameter ( $CD$ , m). The  $CD$  was computed by the average diameter measured in the north–south (crown length— $CL$ , m) and east–west (crown width,  $CW$ , m) directions. The crown projection area ( $CPA$ ,  $m^2$ ) was calculated by  $CPA = \pi CD^2 / 4$ , where  $CD$  = crown diameter and  $\pi = 3.141593$  (Figure 2).

### 2.2.3 | Leaf area index

Another growth parameter determined in the field was the leaf area index ( $LAI$ ,  $m^2 m^{-2}$ ), which was

estimated by the indirect method of light interception using a ceptometer (Accupar LP-80, Decagon Devices, Inc., USA). For this purpose, four reference readings were taken to obtain the incident photosynthetically active radiation (PAR) above the canopy, with eight readings taken under the crown every 30 cm parallel to the rows to obtain the mean PAR under the crown (Figure 2).

### 2.3 | Micrometeorological monitoring

As with all crops, environmental conditions directly influence the productive, morphological and physiological performance of plants. For ‘Kent’ mango, variables such as solar radiation, air temperature, relative humidity and water availability affect productivity, water

consumption, the duration of the phenological phases and the quality and colour of the fruits.

Thus, for this study, the micrometeorological variables were monitored by means of sensors installed on a tower, 8 m in height, placed inside the orchard (Figures 1 and 2). The following variables were measured: incident global solar radiation ( $R_g$ ,  $W m^{-2}$ ), surface-reflected radiation ( $R_r$ ,  $W m^{-2}$ ), downward atmospheric long-wave radiation ( $R_a$ ,  $W m^{-2}$ ), outgoing surface-emitted long-wave radiation ( $R_s$ ,  $W m^{-2}$ ), dry bulb temperature ( $T_{db}$ , °C), wet bulb temperature ( $T_{wb}$ , °C), air temperature ( $T_{air}$ , °C), relative humidity ( $RH$ , %), soil heat flux ( $G$ ,  $W m^{-2}$ ), rainfall ( $R$ , mm) and soil moisture ( $SM$ ,  $cm^3 cm^{-3}$ ). Details of the sensors are shown in Table S2. Each sensor was connected to a data acquisition system (model CR5000, Campbell Scientific Inc., Logan, Utah, USA) that was programmed to take measurements every 30 s and store the mean values at intervals of 30 min. We computed the vapour pressure deficit ( $VPD$ , kPa) following Allen et al. (1998). Monitoring occurred from 10 June 2017 to 7 November 2017 (150 days) in the 2016/2017 cycle and from 8 November 2017 to 20 October 2018 (346 days) in the 2017/2018 cycle. These variables will be used for estimating radiation and energy balances, as well as evapotranspiration and crop coefficients. Furthermore, monitoring rainfall, irrigation and soil moisture will guarantee the best water conditions for orchard performance.

## 2.4 | Radiation balance (RB) and energy balance (EB)

The net radiation represents the energy retained and used by surface biophysical processes ( $R_n$ ,  $W m^{-2}$ ) and was obtained by summing the differences between the radiation that arrived and that left the surface in the form of short and long waves, as per the following equation:

$$R_n = (R_g - R_r) + (R_a - R_s) \quad (1)$$

where  $R_g$  = global solar radiation or surface-incident short-wave radiation,  $W m^{-2}$ ;  $R_r$  = surface-reflected short-wave radiation,  $W m^{-2}$ ;  $R_a$  = downward atmospheric long-wave radiation,  $W m^{-2}$ ; and  $R_s$  = outgoing surface-emitted long-wave radiation,  $W m^{-2}$ .

From the values of  $R_g$  and  $R_r$ , the reflection coefficient or albedo ( $\alpha$ ) of the surface was calculated and is expressed as a percentage:

$$\alpha = \frac{R_r}{R_g} \times 100. \quad (2)$$

The energy balance (EB) was obtained by partitioning the radiation balance ( $R_n$ ) between the processes of

evapotranspiration (latent heat flux— $LE$ ), air heating (sensible heat flux— $H$ ) and soil heating (heat flux of soil— $G$ ), as in the following equation:

$$R_n = LE + H + G \quad (3)$$

where  $LE$  = the latent heat flux,  $W m^{-2}$ ;  $H$  = the sensible heat flux,  $W m^{-2}$ ; and  $G$  = the soil heat flux,  $W m^{-2}$ .

The  $LE$  flux and  $H$  flux were estimated using the energy balance based on the original Bowen ratio (Bowen, 1926), as shown below:

$$LE = \frac{R_n - G}{1 + \beta} \quad (4)$$

$$H = \frac{\beta(R_n - G)}{1 + \beta} \quad (5)$$

where  $\beta$  = the Bowen ratio (dimensionless).

The  $\beta$  parameter is responsible for relating micrometeorological variables to the energy available for the  $LE$  and  $H$  processes. The values were obtained by the original Bowen method, according to Equation (6), and from the model proposed by Lin et al. (2016), Equation (7), considering the air temperature and relative humidity data, when the results of the values of the original Bowen were inconsistent, according to the method of Perez et al. (1999). The validation of the method of Lin et al. (2016) compared to the original Bowen method is shown in Figure 3 for latent ( $LE$ ) and sensible ( $H$ ) heat fluxes, computed by using  $\beta_{Original}$  and  $\beta_{Lin}$ .

$$\beta_{Original} = \gamma \left( \frac{\Delta T}{\Delta e} \right) \quad (6)$$

$$\beta_{Lin} = 1.46 \left( \frac{1}{RH} \right) \left( \frac{T}{273} \right)^2 \exp \left[ -19.83 \left( 1 - \frac{273}{T} \right) \right] \quad (7)$$

where  $\gamma$  is a psychrometric constant ( $kPa \text{ } ^\circ C^{-1}$ );  $\Delta T$  is the air temperature gradient between two profiles above the plant canopy (°C);  $\Delta e$  is the water vapour partial pressure gradient between two profiles above the plant canopy (kPa);  $RH$  is the relative humidity (decimal); and  $T$  is the air temperature (K).

The mean value for each component of the radiation balance and energy balance was recorded at 30 min intervals ( $W m^{-2}$ ) and included in the daily totals in  $MJ m^{-2}$ . The mean values per phenological phase were then calculated considering the two production cycles evaluated in this study.

For a few days during the 2017–2018 cycle, due to problems in the power system of the tower, it was

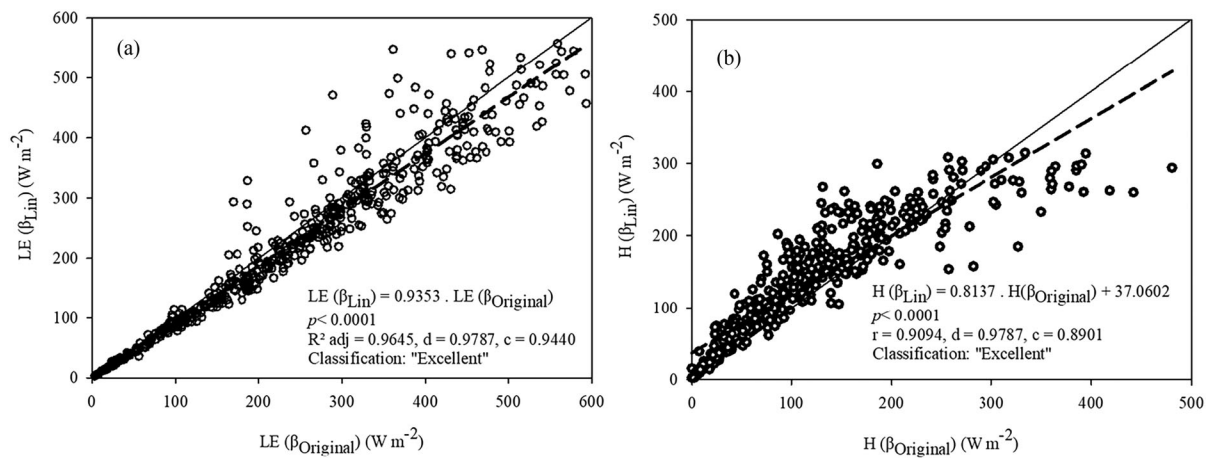


**FIGURE 3** Validation of the data of latent heat flux ( $LE$ ) and sensible heat flux ( $H$ ) estimated by the method of Lin et al. (2016) compared to the data of  $LE$  and  $H$  calculated by Bowen method. Where:  $r$ —correlation coefficient of Pearson,  $d$ —Willmott index of agreement,  $c$ —performance of the method, and the classification, according Souza et al. (2022).

necessary to fill the gaps of 15% of the data from the study period to obtain a continuous and detailed time series of the variables to provide concise results. Furthermore, although the absence of data does not compromise processing, some phases are short in duration and are penalized. The air temperature, air relative humidity, incident solar radiation, wind speed and rainfall data were estimated using correlation equations ( $p < 0.05$ ) obtained by the relationship between the measurements taken in the tower and measurements taken by the agrometeorological station of Embrapa Semiárido located at the Fazenda Andorinhas Farm and, as a second option, with measurements taken by the Salitre Agrometeorological Station (<http://www.cpatas.embrapa.br:8080/servicos/dadosmet/estacoes/index.html>). To fill the gaps in the components of the radiation balance ( $R_n$ ,  $R_r$ ,  $R_a$  and  $R_s$ ), significant correlation equations ( $p < 0.05$ ) between these and the values for  $R_g$  measured by the micrometeorological tower were applied. After filling the gaps, the result was a continuous database of all the environmental parameters necessary to calculate  $LE$  and  $H$ , as well as to determine the  $ET_c$  on a 30-min scale.

## 2.5 | Evapotranspiration and crop coefficient

The crop evapotranspiration ( $ET_{c30min}$ , mm) was estimated every 30 min based on the values for  $LE$ , as per the following expression:

$$ET_{c30min} = \frac{LE \times t \times f_{time}}{L} \quad (8)$$

where  $LE$  = latent heat flux ( $W m^{-2}$ );  $t$  = range of the stored mean values (30 min);  $f_{time}$  = time scale adjustment factor (60 s); and  $L$  = latent heat of vaporization ( $J kg^{-1}$ ).

From the mean 30-min  $ET_c$  values, the daily  $ET_c$  was obtained, considering the period of the day when  $R_n - G > 0$ :

$$ET_{cdaily} = \sum_{R_n - G > 0}^{i=1} ET_{c30min} \quad (9)$$

The reference evapotranspiration ( $ET_0$ , mm) was estimated following the Penman–Monteith method parameterized by FAO Bulletin 56 (Allen et al., 1998) using data from the meteorological station of Embrapa Semiárido located 5 km from the study orchard. Thus, from the relationship between  $ET_c$  and  $ET_0$ , the crop coefficient ( $K_c$ , dimensionless) was calculated relative to each phenological phase of the mango (Table 1), as per the following equation:

$$K_c = \frac{ET_c}{ET_0} \quad (10)$$

## 2.6 | Soil water conditions

To indicate the variation in soil moisture and water availability for the crop, the soil water conditions were analysed by the effective saturation ( $w$ , Equation 11) and the  $f$  factor of the crop ( $f$ , Equation 12):

$$w = \frac{\theta_a - \theta_r}{\theta_s - \theta_r} \quad (11)$$

where  $w$  = effective saturation or relative soil water content (dimensionless);  $\theta_a$  = actual soil moisture ( $SM$ ,  $\text{cm}^3 \text{cm}^{-3}$ ), measured according to Section 2.3;  $\theta_r$  = residual soil moisture, obtained through the retention curve ( $\theta_r$ ,  $\text{cm}^3 \text{cm}^{-3}$ ); and  $\theta_s$  = soil saturation moisture ( $\theta_s$ ,  $\text{cm}^3 \text{cm}^{-3}$ ).

$$f = 1 - w \quad (12)$$

where  $f$  = the  $f$  factor or permissible reduction in soil water availability (dimensionless) and  $w$  = the effective saturation or relative soil water content (dimensionless).

## 2.7 | Data analysis and statistical procedure

All the data were imported and organized into a Microsoft Excel spreadsheet. The 30-min data were converted into daily data. The average, totals and standard deviations for each phenological stage were computed. The graphic representation was made using SigmaPlot 14 software.

## 3 | RESULTS

### 3.1 | Environmental conditions

Figure 4 shows the environmental variables found during the two crop production cycles. The air temperature was higher during November and December ( $31.6^\circ\text{C}$ ), with the lowest values observed in June and July ( $20.2^\circ\text{C}$ ) during the vegetative growth and fruit drop phases, respectively, which favoured subsequent inflorescence growth. The relative humidity reached a maximum value of 87% during the period with the highest rainfall indices, which also coincided with the lowest values for the  $VPD$ . The rainfall ( $R$ ) was 97 mm for the entire period of the experiment, while the total irrigation depth applied was 1857 mm. The highest values of soil moisture ( $\sim 0.12 \text{ cm}^3 \text{ cm}^{-3}$ ) were recorded in the cycle transition (at the end of the fruit formation and maturation phase and at the beginning of the vegetative period), while the lowest averages occurred in the flowering period ( $\sim 0.06 \text{ cm}^3 \text{ cm}^{-3}$ ) due to the adoption of water management for flower induction.

### 3.2 | Phenology and crop growth

There was little variation in the biometric mean values (plant height, crown length, crown width and leaf area

index) (Table 2). Each growth variable increased in value until the fruit-drop phase, with a reduction during the following phase (fruit formation + fruit maturation). During the vegetative phase, the plants had an average height of  $3.4 \pm 0.6$  m, which increased to  $3.5 \pm 0.6$  m at the fruit drop stage. The length of the crown increased from  $2.7 \pm 0.7$  to  $3.0 \pm 0.7$  m, whereas the width of the crown increased from  $4.0 \pm 0.5$  to  $4.2 \pm 0.5$  m for the vegetative and fruit drop stages, respectively. This resulted in a mean crown projection area of  $12.9 \pm 1.7 \text{ m}^2$  throughout the study period. The leaf area index had an overall mean value of  $5.5 \pm 1.4 \text{ m}^2 \text{ m}^{-2}$ , with an apparent reduction of  $1.86 \text{ m}^2 \text{ m}^{-2}$  between the vegetative growth phase and the fruiting phase.

### 3.3 | Radiation balance and energy balance

The daily mean values for the radiation balance components are shown in Figure 5a. The global solar radiation ( $R_g$ ) fluctuates over time, with an emphasis on the rainy season (from January to April) ( $15\text{--}27 \text{ MJ m}^{-2} \text{ day}^{-1}$ ), which afforded intense oscillation due to high cloud concentrations during the summer months in the southern hemisphere, even with no rainfall (Figure 4b). The lowest values of  $R_g$  were found between June and July (the end of autumn to the beginning of the winter season), ranging from 12 to  $20 \text{ MJ m}^{-2}$ , while the maximum values (close to  $30 \text{ MJ m}^{-2}$ ) occurred from October to February (spring to summer).

Figure 5b shows the daily totals for net radiation ( $R_n$ ), latent heat flux ( $LE$ ), sensible heat flux ( $H$ ) and soil heat flux ( $G$ ) in the irrigated mango orchard. The greatest availability of energy ( $R_n$ ) for biophysical processes is seen in the transition of cycles, more specifically, between the end of the fruit formation + maturation phase (FF + MF), vegetative growth (VG) and floral induction (FI), in the following order. At this time, the incidence of sunlight in the region is more intense. On the other hand, this role is reversed during the induction + flowering (FI + FL) and fruit drop (FD) phases (a period characterized by winter in the region). Regarding the performance of biophysical processes, with the exception of  $G$ , which presented less intense values throughout the study, the behaviour of the variables responded to fluctuations in  $R_g$ .  $LE$  was superior to the other types of flux densities during all phenological phases.

Table 3 shows the average values of the components during each phenological phase.  $LE$  presented an average of  $8.5 \pm 1.4 \text{ MJ m}^{-2} \text{ day}^{-1}$ , while  $H$  and  $G$  were more discrete ( $4.1 \pm 0.6$  and  $-0.4 \pm 0.1 \text{ MJ m}^{-2}$ , respectively).



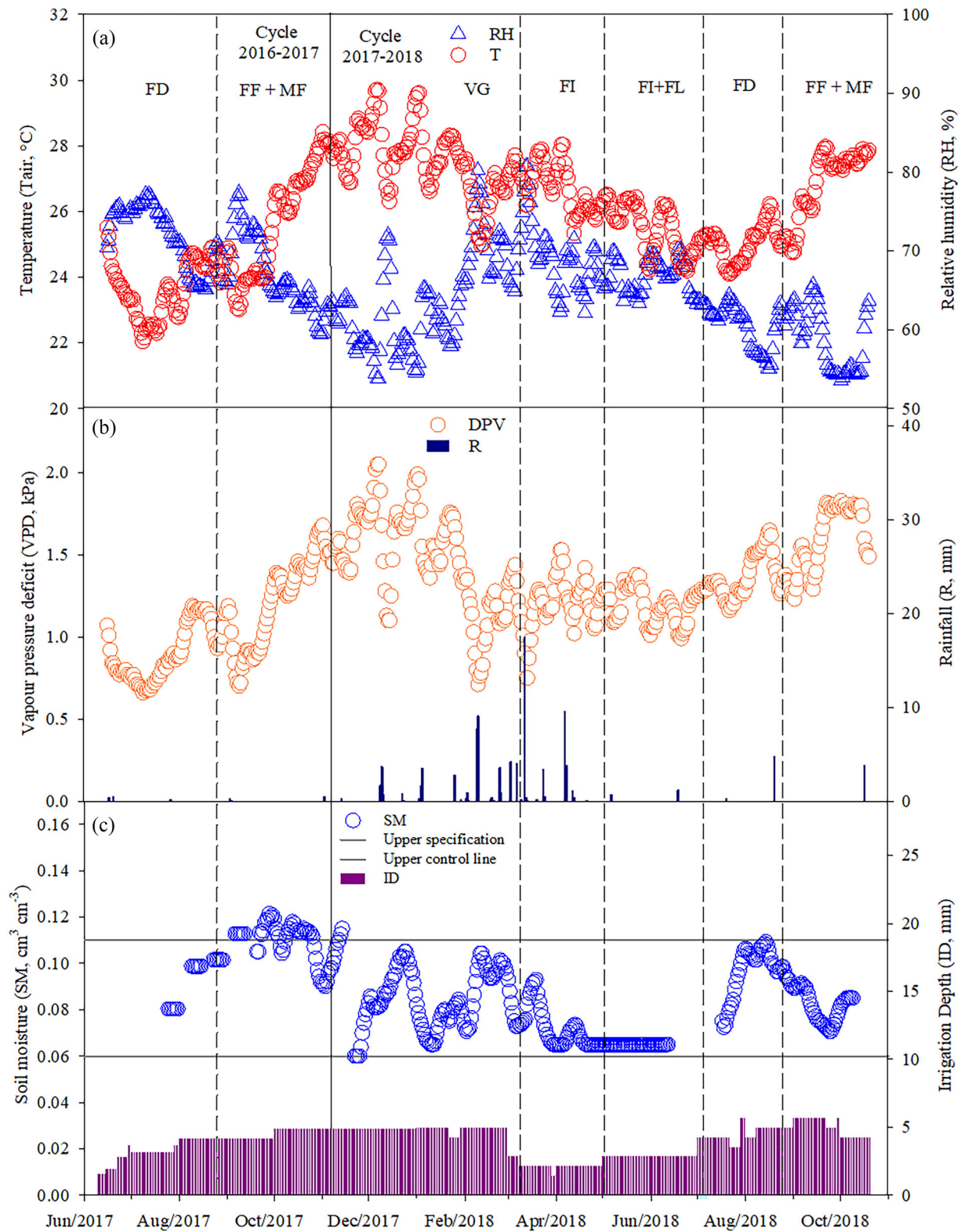


**FIGURE 4** Daily mean values of the environmental variables observed in an orchard of the 'Kent' mango grown in the lower-middle São Francisco valley. FD, fruit drop; FF + MF, fruit formation + fruit maturation; FI, floral induction; FI + FL, floral induction + flowering; VG, vegetative growth.

**TABLE 2** Biometric parameters and leaf area index (LAI) for the phenological phases of a 'Kent' mango orchard grown in the lower-middle São Francisco valley.

Phenology	Plant height (m)	Crown length (m)	Crown width (m)	Crown projection area (m <sup>2</sup> )	LAI (m <sup>2</sup> m <sup>-2</sup> )
Vegetative growth	3.4 ± 0.6	2.7 ± 0.7	4.0 ± 0.5	12.7 ± 1.7	6.5 ± 0.9
Floral induction	3.4 ± 0.6	2.6 ± 0.7	4.0 ± 0.5	12.7 ± 1.5	5.5 ± 1.5
Floral induction + flowering	3.4 ± 0.5	2.7 ± 0.6	4.2 ± 0.5	13.1 ± 1.6	5.9 ± 0.6
Fruit drop	3.5 ± 0.6	3.0 ± 0.7	4.2 ± 0.5	13.1 ± 1.6	5.3 ± 0.4
Fruit formation + fruit maturation	3.3 ± 0.7	2.7 ± 0.8	4.2 ± 0.7	13.1 ± 2.1	4.7 ± 2.0
Mean	3.4 ± 0.6	2.7 ± 0.7	4.1 ± 0.5	12.9 ± 1.7	5.5 ± 1.4

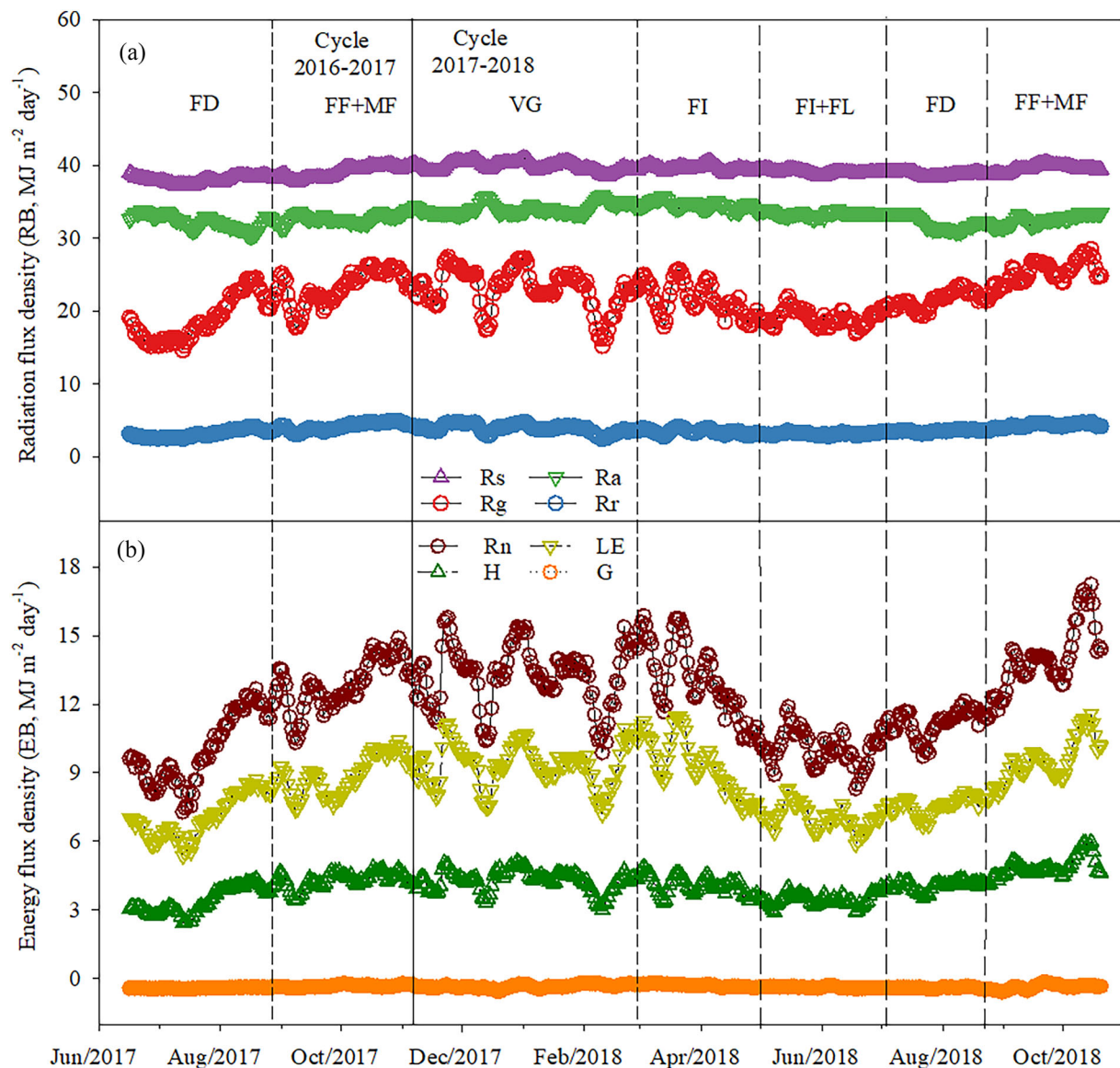


**FIGURE 5** Seasonal variation in radiation (RB) and energy (EB) balance components during the phenological phases of the irrigated 'Kent' mango grown in the São Francisco valley. FD, fruit drop; FF + FM, fruit formation + fruit maturation; FI, floral induction; FI + FL, floral induction + flowering; G, soil heat flux; H, sensible heat flux; LE, latent heat flux;  $R_a$ , atmospheric long-wave radiation;  $R_g$ , atmospheric short-wave radiation;  $R_n$ , net radiation;  $R_r$ , surface reflected short-wave radiation;  $R_s$ , surface-reflected long-wave radiation; VG, vegetative growth.

**TABLE 3** Components of the radiation balance (RB) and albedo ( $\alpha$ ), and components of the energy balance (EB) and Bowen ratio ( $\beta$ ) in an irrigated orchard of the 'Kent' mango in the lower-middle São Francisco valley.

Phenological phase	Radiation balance components (RB, MJ m <sup>-2</sup> day <sup>-1</sup> )				$\alpha$ (%)
	$R_g$	$R_r$	$R_a$	$R_s$	
Vegetative growth	23.0 ± 2.8	3.9 ± 0.6	34.1 ± 0.7	39.8 ± 0.6	17 ± 1
Floral induction	21.5 ± 2.2	3.4 ± 0.3	34.5 ± 0.5	39.6 ± 0.4	16 ± 0
Floral induction + flowering	19.0 ± 1.1	3.1 ± 0.2	33.4 ± 0.3	39.0 ± 0.3	16 ± 0
Fruit drop	20.1 ± 2.1	3.3 ± 0.3	32.2 ± 1.0	38.4 ± 0.4	16 ± 0
Fruit formation + fruit maturation	24.2 ± 2.0	4.2 ± 0.4	32.7 ± 0.6	39.3 ± 0.6	17 ± 0
Cycle	21.8 ± 3.1	3.7 ± 0.6	33.2 ± 1.1	39.2 ± 0.8	17 ± 1
Phenological phase	Energy balance components (EB, MJ m <sup>-2</sup> day <sup>-1</sup> )				$\beta$
	$R_n$	$G$	$LE$	$H$	
Vegetative growth	13.3 ± 1.4	-0.4 ± 0.1	9.4 ± 0.9	4.3 ± 0.5	0.47 ± 0.04
Floral induction	13.0 ± 1.6	-0.3 ± 0.1	9.3 ± 1.2	4.1 ± 0.4	0.45 ± 0.04
Floral induction + flowering	10.0 ± 0.7	-0.4 ± 0.0	7.0 ± 0.5	3.4 ± 0.2	0.49 ± 0.03
Fruit drop	10.6 ± 1.0	-0.4 ± 0.0	7.3 ± 0.7	3.7 ± 0.4	0.53 ± 0.03
Fruit formation + fruit maturation	13.4 ± 1.3	-0.4 ± 0.1	9.2 ± 0.9	4.6 ± 0.4	0.50 ± 0.04
Cycle	12.1 ± 1.9	-0.4 ± 0.1	8.5 ± 1.4	4.1 ± 0.6	0.49 ± 0.05

Note: Mean values followed by the standard deviation ( $\pm$ ).

Abbreviations:  $G$ , soil heat flux;  $H$ , sensible heat flux;  $LE$ , latent heat flux;  $R_a$ , incident long-wave radiation;  $R_g$ , incident short-wave radiation;  $R_n$ , net radiation;  $R_r$ , reflected short-wave radiation;  $R_s$ , reflected long-wave radiation;  $\alpha$ , albedo;  $\beta$ , Bowen ratio.

The ratios of  $LE$  and  $H$  to  $R_n$  were 68 and 32%, respectively. The Bowen ratio ( $\beta$ ) values did not show significant variation between the phenological phases ( $0.53 \pm 0.03$  and  $0.45 \pm 0.04$ ; fruit drop and floral induction, respectively).

Table 3 also confirms that with respect to the radiation balance, the highest and lowest values of latent heat flux ( $LE$ ), sensible heat flux ( $H$ ) and net radiation ( $R_n$ ) were found during the fruit formation + maturation and flowering phases, whereas the highest value of  $LE/R_n$  was found during the vegetative growth phase (71%).

### 3.4 | Evapotranspiration and crop coefficient

The daily and cumulative seasonal values of reference evapotranspiration ( $ET_0$ ), as well as the mango crop evapotranspiration ( $ET_c$ ) and the sum of the precipitation and irrigation depth ( $R + ID$ ), are shown in Figure 6a and Table 4. The  $ET_0$  values varied between 1.47 and 8.29 mm day<sup>-1</sup>, with a mean value of 4.91 ± 1.4 mm day<sup>-1</sup>. The highest  $ET_0$  values were detected between FF + MF (6.09 mm day<sup>-1</sup>) and VG (5.47 mm day<sup>-1</sup>), the period with the greatest insolation. FI, FI + FL and FD were 4.42, 4.08 and 4.51 mm day<sup>-1</sup>, respectively.

The behaviour of  $ET_c$  was similar to that of  $ET_0$ , with higher values in FF + MF (4.46 mm day<sup>-1</sup>) and VG (4.40 mm day<sup>-1</sup>); however, during FI, high values were also observed (4.29 mm day<sup>-1</sup>). The other phases obtained averages close to 3.48 mm day<sup>-1</sup> (FI + FL) and 3.63 mm day<sup>-1</sup> (FD).

The water replacement depth ( $R + ID$ ) has a maximum value of approximately 19.63 mm in the rainy season. Throughout the cycle, the crop presented an accumulated  $ET_c$  (1503 mm) that was slightly lower than the accumulated  $R + ID$  (1506 mm), with the exception of the daily values of flowering phases 1 and 2.

The cultivation coefficient results are presented in Figure 6b and Table 4. From the seasonal behaviour of  $K_c$ , an average value of  $0.83 \pm 0.15$  was derived, ranging from 0.42 to 1.42 during the fruiting phase and vegetative growth phase, respectively. The large difference between  $ET_0$  and  $ET_c$  during the fruiting phase (Figure 6a) led to a reduction in  $K_c$  values in the mango. A similar situation occurred during the fruiting and maturation phases of the 2016–2017 cycle.

Analysing each phenological phase (Table 4), it was verified that the highest average values of  $ET_0$  (6.09 mm) and  $ET_c$  (4.46 mm) occurred during the formation + maturation phase of the fruit, when  $K_c$  was the smallest of all phases (0.74). The phases of VG, FI, FI + FL and FD had average  $K_c$  values of 0.80, 0.97, 0.85 and 0.80, respectively.



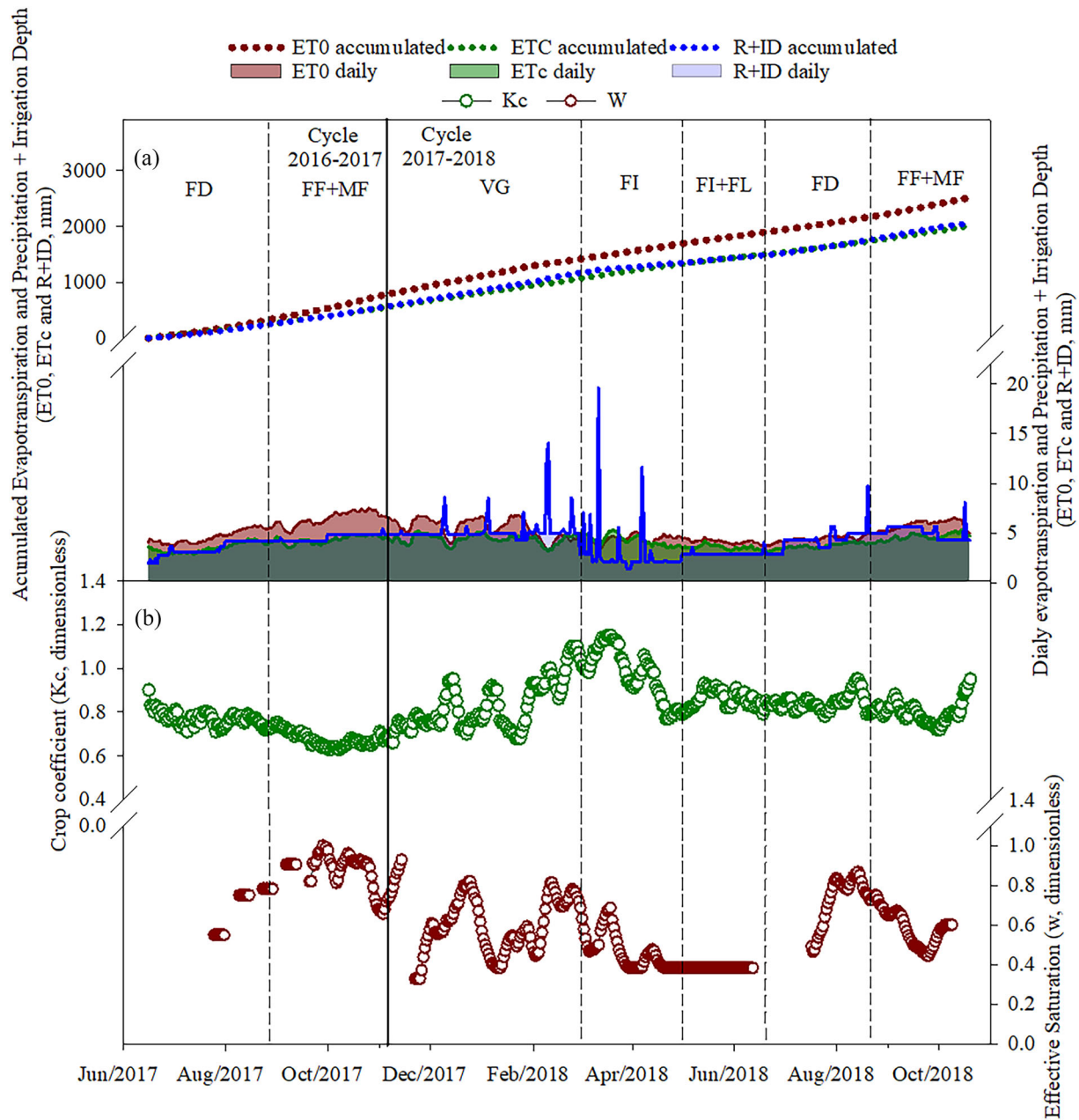


**FIGURE 6** Reference evapotranspiration ( $ET_0$ ), crop evapotranspiration ( $ET_c$ ), precipitation + irrigation depth ( $P + ID$ ), crop coefficient ( $K_c$ ) and effective saturation ( $w$ ) of the irrigated 'Kent' mango in the lower-middle São Francisco valley. FD, fruit drop; FF + MF, fruit formation + fruit maturation; FI, floral induction; FI + FL, floral induction + flowering; VG, vegetative growth.

### 3.5 | Soil water conditions

Effective saturation data ( $w$ ) are shown in Figure 6b. Maximum  $w$  values ( $\sim 0.9$ ) are observed during fruit formation + fruit maturation (FF + MF) for the 2016–2017 cycle and during vegetative growth (VG) and the end of the fruit drop period (FD) in the 2017–2018 cycle.  $w$  values close to 0.4 were found for nearly the entire range of flowering phases (FL1 and FL2). This is reflected in the permissible reduction in water availability ( $f$ )

(Table 4), where water management for floral induction provided significant mean reductions in soil water storage ( $\sim 0.6$ ) in FL1 and FL2. In the other phases, the reductions were less than 39%.

## 4 | DISCUSSION

Among the biometric variables, canopy width and canopy projection area exhibited similar patterns, increasing

**TABLE 4** Reference evapotranspiration ( $ET_0$ ), crop evapotranspiration ( $ET_c$ ), crop coefficient ( $K_c$ ), precipitation + irrigation depth ( $P + ID$ ) and factor  $f$  ( $f$ ) in the irrigated 'Kent' mango in the lower-middle São Francisco valley.

Safra	Phenology	No. days	$ET_0$ (mm day <sup>-1</sup> )	$\sum ET_0$ (mm)	$ET_c$ (mm day <sup>-1</sup> )	$\sum ET_c$ (mm)	$K_c$	$\sum P + LI$ (mm)	$f$
2016–2017	Vegetative growth	–	–	–	–	–	–	–	–
	Floral induction	–	–	–	–	–	–	–	–
	Floral induction + flowering	–	–	–	–	–	–	–	–
	Fruit drop	77	4.56	351	3.49	269	0.77	242	0.33
	Fruit formation + fruit maturation	74	6.40	474	4.32	320	0.68	336	0.13
2017–2018	Vegetative growth	114	5.47	624	4.40	502	0.80	594	0.39
	Floral induction	60	4.42	265	4.29	257	0.97	175	0.54
	Floral induction + flowering	62	4.08	253	3.48	216	0.85	179	0.62
	Fruit drop	52	4.47	232	3.77	196	0.84	237	0.27
	Fruit formation + fruit maturation	59	5.77	341	4.59	271	0.80	299	0.41
Mean	Vegetative growth	114	5.47	624	4.40	502	0.80	594	0.39
	Floral induction	60	4.42	265	4.29	257	0.97	175	0.54
	Floral induction + flowering	62	4.08	253	3.48	216	0.85	179	0.62
	Fruit drop	65	4.51	292	3.63	232	0.80	239	0.30
	Fruit formation + fruit maturation	67	6.09	407	4.46	295	0.74	318	0.27
	Mean/sum	367	4.91	1841	4.05	1503	0.83	1506	0.42

until the floral induction phase and stabilizing after flowering. However, plant height and crown length increased until the fruit drop phase but decreased during the following phase (fruit formation + fruit maturation). This reduction could be observed during fruiting as the developed fruit pulled the branches downwards, causing the crown to open further, resulting in a greater incidence of radiation inside the crown. This interferes with the measurement of radiation below the canopy, promoting a reduction in the leaf area index. In this case, it is important to highlight that the reduction was not due to the mango tree losing its leaves but rather because they were concentrated on the edge of the canopy, influencing the  $LAI$  values. This phenomenon causes the structure of the plant to resemble open-crown pruning or calice, where central branches with an angle of less than 45° are eliminated to favour the passage of light through the canopy (Mouco & Albuquerque, 2015). In studies involving different types of canopy architecture of the 'Tommy Atkins' mango, Espínola Sobrinho (2003) reported that, in addition to promoting greater radiation distribution, the opening of the canopy positively influences the productivity and quality of mango fruit. For the goblet-type format, for example, the authors obtained the lowest albedo values, together with a productivity greater than 40% when combined with the control.

Knowledge of this information is essential since energy interception directly influences the processes of

evapotranspiration ( $LE$ ), air ( $H$ ) and soil heating ( $G$ ). Azevedo et al. (2003) mentioned that the ideal leaf area for satisfactory crop production depends on the cultivar and the number of leaves during sprouting and fruiting. Souza et al. (2018) and Teixeira, Bastiaanssen, Moura, et al. (2008) studied the Tommy Atkins cultivar and reported mean  $LAI$ s of 6.7 and 5.6 m<sup>2</sup> m<sup>-2</sup>, respectively.

The components of the radiation balance show variations throughout each crop cycle as a function of the variation in radiation intensity due to clouds and the angle of incidence of sunlight. According to Souza et al. (2018), the cloud concentration greatly lowers the net radiation, reducing the energy used by biophysical processes. The main component of the radiation balance is  $R_g$ , the value of which directly influences the reflected short-wave radiation ( $R_r$ ) and net radiation ( $R_n$ ), in addition to its effects on air temperature (Figure 5). The greater intensity of solar radiation during the fruit maturation phase favours the levels of sugar and ascorbic acid (Teixeira & Lima Filho, 2004). However, it is worth noting that excess radiation can damage the colour, causing burning of the mango peel (Mouco & Albuquerque, 2015).

The values for  $LE$  were greater than those for the other types of fluxes throughout the cycle. This trend is normal in irrigated crops since water availability allows most of the available energy to be directed to the process of evapotranspiration (Souza et al., 2018). However, the sensible heat flux ( $H$ ) showed no marked fluctuations,

and the values for  $G$  were less intense than those for  $LE$  and  $H$  due to the high vegetation cover and twice-daily irrigation events. According to Lima et al. (2012), the shape of the canopy can directly affect the amount of radiation intercepted by the crop, which affects  $G$  dynamics. In mango plants with an  $LAI$  greater than  $5.0 \text{ m}^2 \text{ m}^{-2}$ , as in the present study, Teixeira, Bastiaanssen, Moura, et al. (2008) reported that  $G$  values change little, demonstrating the efficiency of solar radiation interception by the canopy.

The ratios of  $LE$  and  $H$  to  $R_n$  were 69 and 33%, respectively, which are similar to the values found by Souza et al. (2018) when analysing energy balance in the 'Tommy Atkins' mango grown in the north-east of Pará during the 2010–2011 harvest. Silva et al. (2007), Teixeira, Bastiaanssen, Ahmad, et al. (2008) and Teixeira, Bastiaanssen, Moura, et al. (2008), analysing the 'Tommy Atkins' mango in the lower-middle São Francisco valley, obtained mean  $LE/R_n$  ratios of 76, 77 and 84%, respectively, indicating that most of the energy was used for evapotranspiration. These ratios differ from those in the present study due to the weather conditions, age of the orchard, characteristics of the variety and the water available in the soil. This can be confirmed during the vegetative growth phase, which coincided with the rainy season, i.e. increases in the amount of water in the soil resulted in higher values of  $LE$ . During this period, the rainfall also resulted in moisture between the crop rows, and as such, the increase in  $LE$  possibly occurred because of the greater evaporation. In fruit orchards where the plants are isolated and irrigation is performed by localized methods, such as drip and microsprinklers, the need for water is almost reduced to that of transpiration, which is why, according to Mantovani et al. (2003), these methods moisten only part of the soil, resulting in reduced evaporation.

As shown by Souza et al. (2018), the principal variations in daily evapotranspiration ( $ET_c$ ) in mangos are determined by the available energy and rainfall events. It is also important to note that the values for  $ET_c$  and  $ET_0$  were similar throughout almost the entire experimental period, except for the fruit formation and maturation phases in both cycles. This implies that during this phase, the crop demand was lower than the atmospheric demand, which resulted in a certain reduction in the  $K_c$  value (Figure 6). Azevedo et al. (2003), using the soil water balance and the energy balance based on the Bowen ratio to determine evapotranspiration in the 'Tommy Atkins' mango, obtained a mean  $ET_c$  of  $4.4 \text{ mm day}^{-1}$ . Other studies reported  $ET_c$  values of  $4.7 \text{ mm day}^{-1}$  (Lopes et al., 2001),  $3.7 \text{ mm day}^{-1}$  (Teixeira, Bastiaanssen, Moura, et al., 2008) and  $4.3 \text{ mm day}^{-1}$  (Silva et al., 2009) for the 'Tommy Atkins' mango in the lower-middle São Francisco valley.

The  $K_c$  varied between 0.42 and 1.42 during the fruiting and vegetative growth phases, respectively. The large difference between  $ET_0$  and  $ET_c$  during the fruiting phase (Figure 6) resulted in a reduction in the  $K_c$  values of the crop. This period of the production cycle was characterized by having the greatest amount of available energy, favouring an increase in the  $ET_0$  and  $ET_c$  values. However, the water demand of the mango crop was not proportional to the atmospheric demand, and the crop may have undergone limitations that may have been physiological due to the high heat and low relative humidity ( $T > 27^\circ\text{C}$ ,  $50 < \text{RH} < 60\%$ , Figure 4), together with a reduction in water in the soil. A similar situation occurred during the fruiting and ripening phases of the 2016–2017 cycle (Figures 3–6). However, the values of the present study do not differ from those found in the literature. The mean values of  $K_c$  in the 'Tommy Atkins' mango variety were 0.71 and 0.91, respectively, according to Azevedo et al. (2003) and Teixeira, Bastiaanssen, Moura, et al. (2008).

The highest mean values for  $ET_0$  (6.09 mm) and  $ET_c$  (4.46 mm) occurred during the fruit formation and maturation phases, indicating the period of greatest water consumption by the crop. However,  $K_c$  had the lowest value among all the phases, with  $ET_c$  representing only 73% of  $ET_0$ . This result can be explained by the high values for  $ET_0$ , where  $>6.09 \text{ mm day}^{-1}$  resulted in a reduction in  $K_c$  values due to increased coupling of the crop with the atmosphere, which limited stomatal conductance and stabilized the  $ET_c$  (Farias et al., 2017; Marin et al., 2016, 2020). This information is especially useful, as the period of fruit formation is considered critical in relation to the water demand, and restrictions on the water supply can reduce fruit weight by up to 20%, compromising crop yield (Coelho et al., 2000).

According to the FAO Bulletin 56, fruit trees up to 3 m high, in places without the influence of cover and frost, have average  $K_c$  of 0.55, 0.90 and 0.65 for the initial, medium and final development phases, respectively (Allen et al., 1998). These values are lower than those found. However, it is important to emphasize that the present study was carried out under semi-arid climate conditions with high atmospheric demand, while the values expressed by FAO 56 represent a general average for the characteristics indicated at the beginning. Azevedo et al. (2003), using the Bowen ratio in a crop of the 'Tommy Atkins' mango in the district of Petrolina, Pernambuco, found  $ET_c$  values during flowering, fruit drop and fruit maturation of 4.1, 4.3 and 4.5 mm, respectively, with a mean value for  $K_c$  of 0.71 for the entire production cycle, whereas Teixeira, Bastiaanssen, Moura, et al. (2008), analysing two complete cycles under the same conditions, found  $ET_0$  values of 3.95 and 4.27 mm,  $ET_c$  values of 3.83 and 3.64 mm and  $K_c$  values of 0.97 and 0.85, respectively.



The effective saturation ( $w$ ) and  $f$  factor ( $f$ ) values showed that the water management adopted during the cycle was satisfactory. Both showed sensitivity to irrigation management, especially when there was a reduction in the water depth applied. Analysing these parameters carefully is important, as they favour management efficiency and provide accurate information for decision making. While the values of  $w$  indicate the real soil moisture conditions, the factor  $f$  represents the fraction of reduction in water availability without causing economic damage to the crop. Therefore, values outside the ideal range may make activity unfeasible. For fruit species, this reduction can range between 30 and 70%, and the higher the values, the more tolerant the crop (Tolentino Júnior, 2022). According to Coelho et al. (2007), the critical limit for reducing water availability in the soil is 67% during the flowering phase. In the present study, the greatest reduction occurred in the FI + FL group (62%). In tropical climate regions, water management is one of the most important techniques in the flowering phase since floral differentiation for production depends on water deficit (Prates et al., 2021). During floral induction, water stress is responsible for paralysing growth and decreasing plant vegetative flow, accelerating branch maturation through ethylene production (i.e. responsible for the maturation of plant organs) and abscisic acid synthesis; in addition, when water stress is applied in a way that does not compromise the physiological performance of the plants, the reduction in the applied water layer enhances induction management, increases productivity and reduces production costs (Faria et al., 2016). Cotrim et al. (2017), after testing the effect of irrigation with controlled water deficit in different phenological phases of a 'Tommy Atkins' mango orchard in the semi-arid region of Bahia, concluded that irrigation had no significant effect on the productivity, water use efficiency, number of fruits or weight of the medium of the fruits.

In this study, the productivity of the orchard was  $41 \text{ Mg ha}^{-1}$ , a value that was higher than those found on most farms in the region, as is the case in the study by Simões et al. (2021), which obtained a maximum productivity of  $36 \text{ Mg ha}^{-1}$  for two cycles simultaneously (Cycles 2016–2017 and 2017–2018). These findings led to the conclusion that the above  $K_c$  values are indicated for the production of the 'Kent' mango in the lower-middle São Francisco valley using a microsprinkler irrigation system with production pruning carried out in the late spring.

## 5 | CONCLUSION

The increase in irrigated fruit production and the need for more efficient water management under semi-arid

climate conditions increase the need for accurate and effective information. This study analysed variations in the radiation and energy balance, evapotranspiration and crop coefficient ( $K_c$ ) of the 'Kent' mango variety as a function of the growth and development of the crop in the lower-middle São Francisco valley, an important fruit-growing hub in Brazil, as a way of proposing a specific and detailed water management strategy to enhance the economic development of the region. From this perspective, we conclude the following:

- Atmospheric short-wave radiation ( $R_g$ ) is mainly responsible for the energy destined for net radiation ( $R_n$ ), which is partitioned between energy balance (EB) components.
- In an irrigated 'Kent' mango orchard in the semi-arid conditions of the São Francisco valley, the latent heat ( $LE$ ) and sensible heat ( $H$ ) fluxes constitute approximately 69 and 33%, respectively, of the  $R_n$ .
- The fruit formation + fruit ripening phase is the period of greatest water demand for the crop, even with the reduction in the leaf area index provided by the opening of the canopy due to the weight of the fruits. At this stage, high reference evapotranspiration values ( $6.09 \text{ mm day}^{-1}$ ) promoted a reduction in  $K_c$  values.
- In the climatic conditions of the São Francisco valley, with production pruning occurring in mid-winter/spring,  $K_c$  values of 0.80, 0.97, 0.85, 0.80 and 0.74 are recommended for the 'Kent' mango during the VG, FI, FI + FL, FD and FF + FM phases, respectively.
- The effective saturation ( $w$ ) and the factor  $f$  ( $f$ ) showed that the water stress management strategy during the FI phase was efficient and did not compromise the productivity of the orchard, which reached an average of  $41 \text{ Mg ha}^{-1}$  (higher than the productivity from farms in the region).

## ACKNOWLEDGEMENTS

The authors would like to thank the Coordenação de Aperfeiçoamento de Pessoal de Nível Superior (CAPES—Finance Code 001) and the Conselho Nacional de Desenvolvimento Científico e Tecnológico (309421/2018-7) for their financial support.

## DATA AVAILABILITY STATEMENT

We can make it available if required.

## ORCID

Thieres George Freire da Silva  <https://orcid.org/0000-0002-8355-4935>

## REFERENCES

- Allen, R.G., Pereira, L.S., Raes, D. & Smith, M. (1998) Crop evapotranspiration—guidelines for computing crop water requirements—irrigation and drainage paper 56. FAO, Rome, 300(9), D05109.
- Alvares, C.A., Stape, J.L., Sentelhas, P.C., de Moraes Gonçalves, J.L. & Sparovek, G. (2013) Köppen's climate classification map for Brazil. *Meteorologische Zeitschrift*, 22(6), 711–728. Available from: <https://doi.org/10.1127/0941-2948/2013/0507>
- ANA (Agência Nacional de Águas). (2021) *Atlas irrigação: uso da água na agricultura irrigada*, 2nd edition, Brasília: ANA. Available from: <https://www.gov.br/ana/pt-br/assuntos/gestao-das-aguas/usos-da-agua/irrigacao> [Accessed 25th January 2024].
- Andrade, V.P.M., Simões, W.L., Dias, N.S., Silva, J.S. & Barbosa, K.V.F. (2023) Gas exchange and postharvest quality of 'Kent' mango subjected to controlled water deficit in semiarid region. *Revista Caatinga*, 36(1), 158–166. Available from: <https://doi.org/10.1590/1983-21252023v36n117rc>
- Azevedo, P.V., Silva, B.B. & Silva, V.P. (2003) Water requirements of irrigated mango orchards in northeast Brazil. *Agricultural Water Management*, 58(3), 241–254. Available from: [https://doi.org/10.1016/S0378-3774\(02\)00083-5](https://doi.org/10.1016/S0378-3774(02)00083-5)
- Barbosa, K.S., Sousa, K.S.M., Souza, C.S.G., Cavalcante, Í.H.L., Silva, V.P. & Pereira, W.B. (2023) Influência da aplicação de bioestimulantes em mangueira cv. Kent na qualidade físico-química dos frutos [Biostimulants application influence in mango tree cv. Kent on the fruits physico-chemical quality]. *Brazilian Journal of Animal and Environmental Research*, 6(2), 1403–1416. Available from: <https://doi.org/10.34188/bjaerv6n2-037>
- Bowen, I.S. (1926) The ratio of heat losses by conductions and by evaporation from any water surface. *Physical Review*, 27(6), 779–787. Available from: <https://doi.org/10.1103/PhysRev.27.779>
- Brazilian Horti & Fruti Yearbook. (2022) Mango. Available from: <http://www.editoragazeta.com.br/produto/anuario-brasileiro-de-horti-fruti-2022/> [Accessed 14th February 2024].
- Calzadilla, A., Rehdanz, K. & Tol, R.S. (2010) The economic impact of more sustainable water use in agriculture: a computable general equilibrium analysis. *Journal of Hydrology*, 384(3–4), 292–305. Available from: <https://doi.org/10.1016/j.jhydrol.2009.12.012>
- Campeche, L.F.D.S., Netto, A.O.A., Sousa, I.F., Faccioli, G.G., da Silva, V.D.P. & Azevedo, P.V.D. (2011) Lisímetro de pesagem de grande porte: desenvolvimento e calibração. *Revista Brasileira de Engenharia Agrícola e Ambiental*, 15(5), 519–525. Available from: <https://doi.org/10.1590/S1415-43662011000500013>
- Coelho, E.F., Coelho Filho, M.A. & Santana, J.A.V. (2008) Resposta da mangueira Tommy Atkins an irrigação em condições semi-áridas. *Ceres*, 55(1), 15–20.
- Coelho, E.F., Coelho Filho, M.A. & Silva, A. J. P. (2007) Irrigação da mangueira nas condições Semiáridas do Nordeste. Embrapa Mandioca e Fruticultura Tropical-Circular Técnica (INFOTECA-E). Available from: [https://www.researchgate.net/publication/263770533\\_irrigacao\\_da\\_mangueira\\_nas\\_condicoes\\_semiaridas\\_do\\_nordeste](https://www.researchgate.net/publication/263770533_irrigacao_da_mangueira_nas_condicoes_semiaridas_do_nordeste) [Accessed 21st January 2021]
- Coelho, E.F., Sousa, V.F., Aguiar Netto, A.D.O. & Oliveira, A. S. (2000) Manejo de irrigação em fruteiras tropicais. Embrapa Mandioca e Fruticultura-Circular Técnica (INFOTECA-E). Available from: <https://www.infoteca.cnptia.embrapa.br/infoteca/handle/doc/640631> [Accessed 27th March 2021].
- Cotrim, C.E., Coelho, E.F., Silva, J.A. & Santos, M.R. (2017) Irrigação com déficit controlado e produtividade de mangueira 'Tommy Atkins' sob gotejamento. *Revista Brasileira de Agricultura Irrigada*, 11(8), 22–29. Available from: <https://doi.org/10.7127/rbai.v11n800728>
- Espinola Sobrinho, J. (2003) Influência do tipo de arquitetura do dossel na absorção de radiação solar, na produtividade e na quantidade do fruto da mangueira. 258 f. Tese (Doutorado em Recursos Naturais) - Universidade Federal de Campina Grande, Campina Grande, PB, 2003.
- Faria, L.N., Soares, A.A., Donato, S.L.R., Santos, M.R. & Casto, L.G. (2016) The effects of irrigation management on floral induction of 'Tommy Atkins' mango in Bahia Semiarid. *Engenharia Agrícola*, 36(3), 387–398. Available from: <https://doi.org/10.1590/1809-4430-Eng.Agric.v36n3p387-398/2016>
- Farias, V.D.D.S., Lima, M.J.A.D., Nunes, H.G.G.C., Sousa, D.D.P. & Souza, P.J.D.O.P. (2017) Water demand, crop coefficient and uncoupling factor of cowpea in the eastern amazon. *Revista Caatinga*, 30(1), 190–200. Available from: <https://doi.org/10.1590/1983-21252017v30n121rc>
- Figueiredo Neto, A., Almeida, F.A. & Cavalcante, I.H. (2017) *Manga maturação, colheita e conservação*, 1st edition. Petrolina: UNIVASF.
- IBGE (Instituto Brasileiro de Geografia e Estatística). (2024) Produção agrícola municipal 2022: Culturas temporárias e perenes. Available from: [www.ibge.org.br](http://www.ibge.org.br) [Accessed 14th February 2024]
- Lima, R.T.D., Souza, P.J.D.O.P.D., Rodrigues, J.C. & Lima, M.J.A.D. (2012) Modelos para estimativa da área foliar da mangueira utilizando medidas lineares. *Revista Brasileira de Fruticultura*, 34(4), 974–980. Available from: <https://doi.org/10.1590/S0100-29452012000400003>
- Lin, K.M., Juang, J.Y., Shiu, Y.W. & Chang, L.F.W. (2016) Estimating the bowen ratio for application in air quality models by integrating a simplified analytical expression with measurement data. *Journal of Applied Meteorology and Climatology*, 55(4), 1041–1048. Available from: <https://doi.org/10.1175/JAMC-D-15-0080.1>
- Lopes, P.M.O., Silva, B.B., Azevedo, P.V., Silva, V., Teixeira, A.D.C., Soares, J.M., et al. (2001) Balanço de energia num pomar de mangueiras irrigado. *Revista Brasileira de Agrometeorologia*, 9(1), 1–8.
- Mantovani, E.C. (2001) *Avalia: Programa de avaliação da irrigação por aspersão e localizada*. Viçosa, MG: UFV, pp. 77–80.
- Mantovani, E.C., Zinato, C.E. & Simão, F.R. (2003) Manejo de irrigação e fertirrigação na cultura da goiabeira. In: Rozane, D.E. & Couto, F.A.A. (Eds.) *Cultura da goiabeira: tecnologia e mercado*. Viçosa: Universidade Federal de Viçosa, pp. 243–302.
- Marin, F.R., Angelocci, L.R., Nassif, D.S., Costa, L.G., Vianna, M.S. & Carvalho, K.S. (2016) Crop coefficient changes with reference evapotranspiration for highly canopy-atmosphere coupled crops. *Agricultural Water Management*, 163, 139–145. Available from: <https://doi.org/10.1016/j.agwat.2015.09.010>
- Marin, F.R., Inman-Bamber, G., Silva, T.G., Vianna, M.S., Nassif, D.S. & Carvalho, K.S. (2020) Sugarcane

- evapotranspiration and irrigation requirements in tropical climates. *Theoretical and Applied Climatology*, 140(3-4), 1349–1357. Available from: <https://doi.org/10.1007/s00704-020-03161-z>
- Mouco, M.A.C. (2015) *Cultivo de mangueira*, 3rd edition. Petrolina: Embrapa Semiárido (Sistemas de Produção, versão eletrônica). Available from: <https://www.infoteca.cnptia.embrapa.br/handle/doc/1031747>
- Mouco, M.A.C. & Albuquerque, J.A.S. (2015) Sistemas de poda. In: Mouco, M.A.C. (Ed.) *Cultivo de mangueira*, 3rd edition. Petrolina: Embrapa Semiárido (Sistemas de Produção, versão eletrônica). Available from: <https://www.infoteca.cnptia.embrapa.br/handle/doc/1031747>
- Pereira, A.R., Sediya, G.C. & Villa Nova, N.A. (2013) *Evapotranspiração*. Campinas-SP: FUNDAG.
- Perez, P.J., Castellví, F., Ibañez, M. & Rosell, J.I. (1999) Assessment of reliability of Bowen ratio method for partitioning fluxes. *Agricultural and Forest Meteorology*, 97(3), 141–150. Available from: [https://doi.org/10.1016/S0168-1923\(99\)00080-5](https://doi.org/10.1016/S0168-1923(99)00080-5)
- Prates, A.R., Züge, P.G.U., Leonel, S., Souza, J.M.A. & Ávila, J. (2021) Flowering induction in mango tree: updates, perspectives and options for organic agriculture. *Pesquisa Agropecuária Tropical*, 51, e68175. Available from: <https://doi.org/10.1590/1983-40632021v5168175>
- Rodrigues, J.C., Souza, P.J.D.O.P.D. & Lima, R.T.D. (2013) Estimativa de temperaturas basais e exigência térmica em mangueiras no nordeste do estado do Pará. *Revista Brasileira de Fruticultura*, 35(1), 143–150. Available from: <https://doi.org/10.1590/S0100-29452013000100017>
- Silva, V.D.P., Garcêz, S.L., Silva, B.B.D., Albuquerque, M.F.D. & Almeida, R.S. (2015) Métodos de estimativa da evapotranspiração da cultura da cana-de-açúcar em condições de sequeiro. *Revista Brasileira de Engenharia Agrícola e Ambiental*, 19(5), 411–417. Available from: <https://doi.org/10.1590/1807-1929/agriambi.v19n5p411-417>
- Silva, V.D.P.R., Azevedo, P.V. & Silva, B.B. (2007) Surface energy fluxes and evapotranspiration of a mango orchard grown in a semiarid environment. *Agronomy Journal*, 99(6), 1391–1396. Available from: <https://doi.org/10.2134/agronj2006.0232>
- Silva, V.D.P.R., Campos, J.H.B.C. & Azevedo, P.V. (2009) Water-use efficiency and evapotranspiration of mango orchard grown in northeastern region of Brazil. *Scientia Horticulturae*, 120(4), 467–472. Available from: <https://doi.org/10.1016/j.scienta.2008.12.005>
- Simões, W.L., Andrade, V.P., Mouco, M.A.C., Souza, J.S.C. & Lima, J.R.F. (2021) Produção e qualidade da mangueira ‘Kent’ (*Mangifera indica* L.) submetida a diferentes lâminas de irrigação no semiárido nordestino. *Revista em Agronegócio e Meio Ambiente*, 14(2), 305–314. Available from: <https://doi.org/10.17765/2176-9168.2021v14n2e7832>
- Simões, W.L., Ferreira, P.P.B., Mouco, M.A.C., Lima, M.A.C., Guimarães, M.J.M. & Silva, J.A.B. (2018) Produção e respostas fisiológicas da mangueira cv. Keitt sob diferentes sistemas de irrigação no Submédio do São Francisco. *Irriga*, 23(1), 34–43. Available from: <https://doi.org/10.15809/irriga.2018v23n1p34>
- Souza, L.S.B., Silva, M.T.L., Alba, E., Moura, M.S.B., Cruz Neto, J.F., Souza, C.A.A., et al. (2022) New method for estimating reference evapotranspiration and comparison with alternative methods in a fruit-producing hub in the semiarid region of Brazil. *Theoretical and Applied Climatology*, 149(1-2), 593–602. Available from: <https://doi.org/10.1007/s00704-022-04069-6>
- Souza, P.J.D.O.P.D., Rodrigues, J.C., Sousa, A.M.L.D. & Souza, E.B.D. (2018) Diurnal energy balance in a mango orchard in the Northeast of Pará, Brazil. *Revista Brasileira de Meteorologia*, 33(3), 537–546. Available from: <https://doi.org/10.1590/0102-7786333012>
- Teixeira, A.D.C., Bastiaanssen, W.G., Moura, M.S.B., Soares, J.M., Ahmad, M.U.D. & Bos, M.G. (2008) Energy and water balance measurements for water productivity analysis in irrigated mango trees, Northeast Brazil. *Agricultural and Forest Meteorology*, 148(10), 1524–1537. Available from: <https://doi.org/10.1016/j.agrformet.2008.05.004>
- Teixeira, A.H.C., Bastiaanssen, W.G., Ahmad, M.U.D., Moura, M.D. & Bos, M.G. (2008) Analysis of energy fluxes and vegetation-atmosphere parameters in irrigated and natural ecosystems of semiarid Brazil. *Journal of Hydrology*, 362(1–2), 110–127. Available from: <https://doi.org/10.1016/j.jhydrol.2008.08.011>
- Teixeira, A.H.C. & Lima Filho, J.M.P. (2004) Clima. In: Mouco, M.A.C. (Ed.) *Cultivo de mangueira*, 2nd edition. Petrolina: Embrapa Semiárido (Sistemas de Produção, versão eletrônica). Available from: [www.cpatsa.embrapa.br:8080/sistema\\_producao/spmanga/index.htm](http://www.cpatsa.embrapa.br:8080/sistema_producao/spmanga/index.htm)
- Tolentino Júnior, J.B. (2022) *Irrigação Pressurizada*. Santa Catarina: Universidade Federal de Santa Catarina Centro de Ciências Rurais. Available from: <https://irrigacao.tolentino.pro.br/>
- Zuazo, V.H.D., Pleguezuelo, C.R.R., Ruiz, B.G., Gordillo, S.G. & Terejo, I.F.G. (2019) Water use and fruit yield of mango (*Mangifera indica* L.) grown in a subtropical Mediterranean climate. *International Journal of Fruit Ciência*, 19(2), 136–150. Available from: <https://doi.org/10.1080/15538362.2018.1493960>

## SUPPORTING INFORMATION

Additional supporting information can be found online in the Supporting Information section at the end of this article.

**How to cite this article:** da Silva, M.J., de Moura, M.S.B., Carvalho, H.F.S., dos Santos, C.V.B., Leitão, Mário de Miranda Villas Boas Ramos, Campeche, L.F.S.M. et al. (2024) Evapotranspiration and crop coefficient of ‘Kent’ mango in an important fruit-growing hub in Brazil. *Irrigation and Drainage*, 1–17. Available from: <https://doi.org/10.1002/ird.2962>